Mem. S.A.It. Suppl. Vol. 19, 158

Memorie della
Supplementi

A comparison between SFR diagnostics and CC SN rate within 11 Mpc.

M.T. Botticella[1], S.J. Smartt[1], R.C. Kennicutt, Jr.[2], E. Cappellaro[3], M. Sereno[4], and J.C. Lee[5]

[1] Astrophysics Research Centre, School of Mathematics and Physics, Queen's University Belfast, Belfast BT7 1NN, UK
[2] Institute of Astronomy, University of Cambridge, Madingley Road, Cambridge CB3 0HA, UK
[3] INAF- Osservatorio Astronomico di Padova, Vicolo dell'Osservatorio 5, 35122 Padova, Italy
[4] Dipartimento di Fisica, Politecnico di Torino, Corso Duca degli Abruzzi 24, 10129, Torino, Italy
[5] Carnegie Fellow, Carnegie Observatories, 813 Santa Barbara Street, Pasadena, CA 91101
e-mail: m.botticella@qub.ac.uk

Abstract. The core collapse supernova (CC SN) rate provides a strong lower limit for the star formation rate (SFR). Progress in using it as a cosmic SFR tracer requires some confidence that it is consistent with more conventional SFR diagnostics. We compare standard SFR measurements based on Hα, Far Ultraviolet (FUV) and Total Infrared (TIR) galaxy luminosities with the observed CC SN rate in the same galaxy sample. The comparison can be viewed from two perspectives. Firstly, by adopting an estimate of the minimum stellar mass to produce a CC SN one can determine a SFR from SN numbers. Secondly, the radiative SFRs can be assumed to be robust and then the SN statistics provides a constraint on the minimum stellar mass for CC SN progenitors. We exploit the multi-wavelength data set from 11HUGS, a volume-limited survey designed to provide a census of SFR in the local Volume. There are 14 SNe discovered in this sample of galaxies within the last 13 years. Assuming a lower limit for CC SN progenitor of 8 $M_{\odot}$, the CC SN rate matches the SFR from the FUV luminosity. However, the SFR based on Hα luminosity is lower than these two estimates by a factor of about 2. If we assume that the FUV or Hα based luminosities are a true reflection of the SFR, we find that the minimum mass for CC SN progenitors is $8 \pm 1\,M_{\odot}$ and $6 \pm 1\,M_{\odot}$, respectively.

Key words. Stars: Supernovae – Galaxy: star formation rate

1. Introduction

The progenitors of CC SNe are massive stars, either single or in binary system, that complete the exothermic nuclear burnings, up to be development of an iron core that cannot be supported by any further nuclear fusion reactions or by electron degenerate pressure. The subsequent collapse of the iron core results into

Send offprint requests to: M.T. Botticella

the formation of a compact object, a neutron star or a black hole, accompanied by the high-velocity ejection of a large fraction of the progenitor mass. Due to the short lifetime of their progenitor stars, the rate of occurrence of CC SNe closely follows the current SFR in a stellar system. The evolution of CC SN rate with redshift is a probe of the SF history and allow us to constrain the chemical enrichment of the galaxies and the effect of energy/momentum feedback by CC SNe, both important ingredient in modeling galaxy formation and evolution. Poor statistics is a major limiting factor for using the CC SN rate as a tracer of the SFR both at low redshift, due the difficulty of sampling large volumes, and at high redshift, due to the difficulty of detecting and typing intrinsically faint SNe (Botticella et al. 2008). Moreover a significant fraction of CC SNe is missed by optical searches, since they are embedded in dusty spiral arms or galaxy nuclei, and this fraction may change with redshift, if the amount and the average properties of dust in galaxies evolve with time. Progress in using CC SN rate as a SFR tracer requires on one hand accurate measurements of rates at various cosmic epochs and in different environments and on the other a meaningful comparison with other SFR diagnostics to verify its reliability and to analyse its main limitations.

The CC SN rate is also a powerful tool to investigate the nature of SN progenitors and to test the stellar evolutionary models. Different sub-types of CC SNe have been identified on the basis of their spectroscopic and photometric properties and a possible sequence has been explained on the basis of the progenitor mass loss history (Heger et al. 2003). However, this simple scheme where only the mass loss drives the evolution of massive stars can not explain the variety of the observational properties showed by CC SNe of the same sub-type and the relative numbers of different sub-types (Smartt 2009). In particular two important issues as what is the minimum mass of a star that leads to a CC SN in a single or binary system and what is the mass range of progenitor stars of different CC SN sub-types have still to be set. It is possible to constrain the mass range of stars that produce CC SNe by comparing the CC SN rate expected for a given SFR and the observed one in the same galaxy sample or in the same volume.

We exploited the multi-wavelength data collected for a volume-limited sample of nearby galaxies to compare different SFR diagnostics with CC SN rate and to constrain the cutoff mass for CC SN progenitors by adopting the SFR as traced by FUV and Hα emission. The novelty of this work consists in studying both CC SN rate and SFR in the same well defined galaxy sample.

2. 11 HUGS Galaxy sample

Our galaxy sample is based upon the statistically complete catalog of the 11 Mpc Hα and Ultraviolet Galaxy Survey (11HUGS). 11HUGS was designed to provide a census of SFR in the Local Volume, to characterize the population of the star forming galaxies and to constrain the temporal behavior of the SF in low mass galaxies. A distance-limit of 11 Mpc[1] of the Milk Way was adopted to simultaneously obtain a sample that is statistically significant and not so incomplete as catalogues at larger distance. Direct stellar distances are available for most galaxies within $\sim$ 5 Mpc of the Milk Way while distances for other galaxies are obtained using the galaxy radial velocity corrected according to the Local Group flow model provided by the Karachentsev & Makarov (1996) and Hubble constant. The design of the 11HUGS survey, its completeness properties, the observations, the data processing and the characteristics of the galaxy sample (436 galaxies) are described in Kennicutt et al. (2008).

Deep, single orbit imaging in the FUV and NUV bands was obtained for 349 galaxies included in the 11HUGS sample following the strategy of the GALEX Nearby Galaxy Survey and full details on GALEX observations and photometry have been provided by Lee et al. (2010). The data from 11HUGS have further been augmented by Spitzer observations

[1] Thorough this work we adopt a Hubble constant of 75 km s^{-1} Mpc^{-1}.

through the composite Local Volume Legacy[2] program and data from the Two Micron All Sky Survey (2MASS). Spitzer MIR (IRAC) and FIR (MIPS) data have been obtained for 180 galaxies and the globally integrated 0.15–160 μm spectral energy distribution is obtained from GALEX, 2MASS, IRAS and Spitzer data (Dale et al. 2009). For our analysis we considered three different samples: 383 galaxies (88% of 11HUGS sample) with measured flux in the Hα (sample A), 312 galaxies (71%) with both measured flux in the Hα and FUV (sample B) and 167 galaxies (38%) with measured flux in Hα , FUV and TIR range (sample C).

2.1. Sample A : Hα luminosities

Integrated Hα luminosities ($L_{\mathrm{H}\alpha}$) are obtained by Kennicutt et al. (2008) after applying the following corrections:

- emission of the [NII] ($\lambda\lambda 6548, 6583$) satellite forbidden lines,
- underlying stellar absorption by subtracting a scaled R band images from the narrow band images,
- Galactic foreground extinction exploiting the relationship between the color excess and extinction ($A_{\mathrm{H}\alpha} = 2.5 \times E(B-V)$ mag) by using values based on the maps of Schlegel et al. (1998) and the Cardelli et al. (1989) extinction law with $R_V = 3.1$.

No correction of Hα fluxes for internal extinction has been applied in the published catalogue. For the $\sim$ 20% of the sample it was possible to estimate the internal dust extinction via the Balmer decrement, since spectroscopic measurements of Hα/Hβ from the literature are available, by assuming a case B recombination ratio and the Cardelli et al. (1989) extinction law with $R_V = 3.1$ and using the following relation between $A_{\mathrm{H}\alpha}$ and Hα/Hβ flux ratio:

$$A_{\mathrm{H}\alpha} = 5.91 \log \frac{f_{\mathrm{H}\alpha}}{f_{\mathrm{H}\beta}} - 2.70 \quad (1)$$

For the galaxies without measurements of the Balmer decrement we adopt an empirical correction scaling with parent galaxy luminosity following the algorithm of Lee et al. (2009):

$$A_{\mathrm{H}\alpha} = 0.10 \quad if M_B > -14.5$$
$$A_{\mathrm{H}\alpha} = 1.971 + 0.323 M_B + 0.0134 M_B^2 \quad if M_B \leq -14.5$$

The SFRs in the sample A have been estimated by adopting the conversion factor by Kennicutt (1998) :

$$SFR(\mathrm{M}_\odot\, yr^{-1}) = 7.9 \times 10^{-42} L_{\mathrm{H}\alpha}(ergs^{-1}) \quad (2)$$

that assumes a Salpeter IMF in the mass range 0.1–100 $\mathrm{M}_\odot$, solar metallicity and a constant SFR for at least the past $\sim$ 10 Myr.

2.2. Sample B: Hα and FUV luminosities

The procedure used to perform FUV and NUV photometry and to measure the FUV luminosity (L_{FUV}) is detailed in Lee et al. (2010). The fluxes have been corrected for Galactic reddening by using the relationship $A_{\mathrm{FUV}} = 7.9 \times E(B-V)$, adopting $E(B-V)$ values based on the maps of Schlegel et al. (1998) and the Cardelli et al. (1989) extinction law. When TIR data are available the correction for internal extinction is obtained by using the mapping between A_{FUV} and the TIR/FUV flux ratio given by Buat et al. (2005):

$$A_{\mathrm{FUV}} = -0.0333x^3 + 0.3522x^2 + 1.1960x + 0.4967 \quad (3)$$

where x=log(TIR/FUV). Lee et al. (2009) compared the Hα and FUV attenuations finding a good correlation with a slope $A_{\mathrm{FUV}}/A_{\mathrm{H}\alpha} = 1.8$ that is the expected value for the Calzetti's obscuration curve and differential extinction law (Calzetti 2001). When TIR data are not available or when the equation gives a negative correction, the A_{FUV} was obtained scaling the computed $A_{\mathrm{H}\alpha}$ by a factor 1.8 (Lee et al. 2009).

The SFRs in the sample B have been estimated by adopting the conversion factors by Kennicutt (1998) that assumes a Salpeter IMF in the mass range 0.1–100 $\mathrm{M}_\odot$, solar metallicity and a constant SFR for at least the past $\sim$ 100 Myr:

$$SFR(\mathrm{M}_\odot\, yr^{-1}) = 1.4 \times 10^{-28} L_{\mathrm{FUV}}(ergs^{-1}Hz^{-1}) \quad (4)$$

[2] http://www.ast.cam.ac.uk/research/lvls/

Table 1. The number of galaxies and CC SNe discovered in the last 13 years, the total $L_{H\alpha}$ (10^{43} erg s^{-1}) and SFR ($M_{\odot}yr^{-1}$) for the three samples we have analysed.

Parameter	A	B	C
N_{gal}	383	312	167
N_{CC}	14	13	12
$L_{H\alpha}$	1.1 ± 0.05	0.9 ± 0.05	0.7 ± 0.04
$SFR_{H\alpha}$	87 ± 4	78 ± 4	58 ± 4
SFR_{FUV}	...	123 ± 8	94 ± 6
$SFR_{H\alpha+TIR}$	...	...	62 ± 4

2.3. Sample C: Hα, FUV and TIR luminosities

In the sample C, in addition to $L_{H\alpha}$ and L_{FUV}, the TIR luminosity (L_{TIR}) is obtained combining Spitzer MIR and FIR fluxes with 2MASS NIR data (Dale et al. 2009)[3]. For a given galaxy, in most cases the same aperture was used for extracting all infrared fluxes. L_{TIR} has been used to obtain reliable extinction corrected SFRs according to the prescription of Kennicutt et al. (2009):

$$SFR(M_{\odot}\, yr^{-1}) = 7.9 \times 10^{-42}(L_{H\alpha} + 0.0024 L_{TIR}) \quad (5)$$

3. 11 HUGS SN sample

To estimate the CC SN rate we initially identified SNe known to have occurred in the galaxies of the Sample A from the Asiago SN catalogue[4] from 1885 to 2010: 38 CC SNe and 10 type Ia SNe. We considered only the CC SNe discovered in the optical searches[5]. There are a further 10 events that have not been spectroscopically classified but are likely SNe of some sort, and an additional faint transient in NGC 4656 discovered in 2005 of unknown origin (Rich et al. 2005). Additionally there have been discoveries of 7 Luminous Blue Variables (LBVs) in outbursts, and two optical transients whose nature is still debated (SN 2008S and NGC 300-2008OT)[6]. A SN origin from a massive star ($> 7 - 8\, M_{\odot}$) has been proposed for SN 2008S (and NGC 300-2008OT by implication) by a number of authors but is disputed by others who favour an outbursting massive star event (Botticella et al. 2009; Pumo et al. 2009, and reference therein). To be conservative, we will not consider these two transients as genuine CC SNe in our main analysis. We restrict our comparison between the CC SN rate and the SFR estimates to the last 13 yr (1998–2010), assuming a constant intensity level of surveillance (i.e. a control time (CT) of 13 years). This period is well justified as since 1998 we have witnessed a large increase in the discovery rate of SNe in the Local Universe due to the start of LOSS SN search in 1998 targeting about 15,000 galaxies with $z < 0.05$ (Leaman et al. 2010) and the high number of amateurs searching SNe in the nearby galaxies who have had been using telescopes of 20-50 cm and modern CCDs. The majority (60% of events) of CC SNe within 11 Mpc in the last 13 years (Table 2) have been discovered by astronomer amateurs: four events were discovered soon after the explosion, six events were discovered either before an unambiguous lightcurve maximum or early in the plateau phase, four events are type IIP SNe discovered during mid-plateau. Early discoveries of two events were missed simply due to the galaxies being in solar conjunction at SN explosion epoch. All of this supports our view that our galaxy samples have been systematically surveyed during the last 13 years, and the CC SN rate is at least reliable enough for a meaningful comparison with the SFR estimates now available. Restricting our SN sample to that discovered in the last 13 years has an other advantage: all of the SNe are spectroscopically classified and the majority have extensive photometric and spectroscopic coverage of their evolution.

[3] with the exception of NGC 628, NGC 1058 and NGC 6949 for which data are from C. Hao (private communication).

[4] http://graspa.oapd.inaf.it/

[5] SN 2008iz was discovered in NGC3034 (M82) in the radio and its SN nature was confirmed with identification of the expanding ring (Brunthaler et al. 2010)

[6] SN 2010da seems to be a LBV-like outburst of a dust enshrouded massive star with bluer colours than those of the progenitors of SN 2008S and NGC 300 OT2008-1.

Table 2. The SN type, magnitude at the discovery epoch and at maximum light, the temporal interval between the discovery epoch and the maximum light, the host galaxy, its morphological type, *B* band absolute magnitude and SFRs for SNe discovered within 11 Mpc in the last 13 yr.

SN	type	mag disc.	mag max.	phase	ref.	gal.	T	M_B	$SFR_{H\alpha}$	SFR_{UV}
2002ap	Ic	14.5 (V)	12.39 (V)	-9	1	NGC 628	5	−19.58	1.3	2
2002bu	IIn	15.5	14.77 (R)	-5	2	NGC 4242	8	−18.18	0.1	0.17
2002hh	IIP	16.5	15.53 (R)	-4	3	NGC 6946	6	−20.79	5.7	9.1
2003gd	IIP	13.2	13.63 (R)	+90	4	NGC 628	5	−19.58	1.3	2
2004am	IIP	17.0	∼16 (R)	+90	5	NGC 3034	7	−18.84	1.9	5.6
2004dj	IIP	11.2	11.55 (R)	+21	6	NGC 2403	6	−18.78	0.8	1.0
2004et	IIP	12.8	12.2 (R)	-18	7	NGC 6946	6	−20.79	5.7	9.1
2005af	IIP	12.8	12.8 (R)	+30	8	NGC 4945	6	−19.26	0.9	–
2005at	Ic	14.3	14.3	0	9	NGC 6744	4	−20.94	3.3	12
2005cs	IIP	16.3 (V)	14.50 (V)	-2	10	NGC 5194	4	−20.63	4.5	7.6
2007gr	Ic	13.8	12.76	-13	11	NGC 1058	5	−18.24	0.3	0.5
2008S	...	16.7 (R)	16.26 (R)	-11	12	NGC 6946	6	−20.79	5.7	9.1
2008ax	IIb	16.1	13.38 (r)	-23	13	NGC 4490	7	−19.37	1.9	2.5
2008bk	IIP	12.6	12.5		14	NGC 7793	7	−18.41	0.5	0.7
2008OT	...	14.3	14.3	0	15	NGC 300	7	−17.84	0.2	0.3
2009hd	IIP	17.2	16 (R)		16	NGC 3627	3	−20.44	2.6	4.9

(1) Nakano et al. (2002); (2) Foley et al. (2003);(3) Pozzo et al. (2006); (4) Hendry et al. (2005); (5) Singer et al. (2004); (6) Vinkó et al. (2006); (7) Maguire et al. (2010); (8) Jacques & Pimentel (2005); (9) Martin et al. (2005); (10) Pastorello et al. (2006); (11) Hunter et al. (2009); (12) Botticella et al. (2009); (13) Pastorello et al. (2008); (14) Monard (2008b); (15) Monard (2008a); (16) Monard (2009).

4. Comparison of SFR indicators

The number of SN discoveries within the 11 Mpc volume now makes for an interesting comparison between the SFRs obtained from the observed CC SN rate and those based on multi-wavelength flux measurements. Each provides an independent measurement which suffers from different uncertainties and biases to the others. The CC SN rate is likely biased towards the brighter SNe and maybe systematically misses a population of SN explosions (due to either modest intrinsic brightness or huge extinction) so it gives a lower limit for the current SFR. Dust extinction is probably the largest source of systematic uncertainty in the direct measurements of SFRs (typical dust attenuation is of order $0-2$ mag in Hα and $0-4$ mag in UV continuum Kennicutt et al. 2009). In order to estimate the SFR from CC SN rate measurements we have to assume the mass range of CC SN progenitors and to correct the rates for the fraction of the extinguished CC SNe that are missed in optical searches. The lower mass limit for CC SN progenitors from direct detections of progenitor stars in high-resolution images has arrived at a best estimate of $8.5^{+1}_{-1.5}\,M_\odot$ (Smartt et al. 2009), which is in reasonable agreement with the most massive WD progenitors (Williams et al. 2009). The current best estimate from these two methods is $8\pm1\,M_\odot$ Smartt (2009). If we assume this value of of $8\,M_\odot$ the observed CC SN rates in the galaxy samples A, B and C imply the SFRs plotted in Fig 1. The SFR from CC SNe is higher by a factor two compared with those in Sample A and C based on $L_{\rm H\alpha}$ while there is good agreement with the SFR based on $L_{\rm FUV}$ that suggests we are not missing a large number of CC SNe within 11 Mpc due to dust extinction. The main source of the difference between the corrected SFRs based

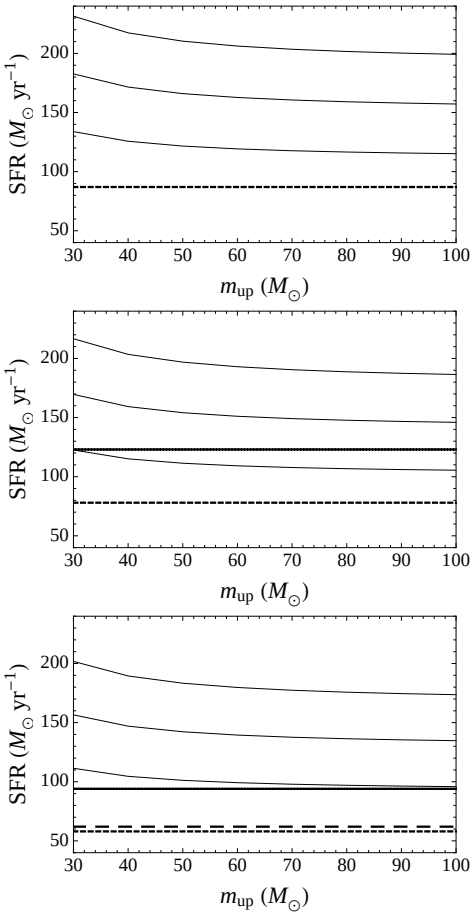

Fig. 1. The SFRs expected in the sample A, B, C as a function of the upper mass limit for CC SN progenitors. These SFRs have been obtained from the observed CC SN rates adopting a lower mass limit of 8 $M_\odot$ for CC SN progenitor mass range. The dotted and black lines are the SFRs based on $L_{\rm H\alpha}$ and on $L_{\rm FUV}$, respectively.

on $L_{\rm FUV}$ and $L_{\rm H\alpha}$ is due likely to the attenuation corrections.

5. Estimate of the CC SN progenitor mass range

Stellar evolutionary models predict a value of minimum mass for the CC SN progenitors in the range 7–11 $M_\odot$ but this prediction is not useful since for a burst of SF assuming a Salpeter IMF the number of stars in this mass range is very similar to the number of stars with mass larger than 11 $M_\odot$. Moreover this value is different for single stars and close binary systems and is quite sensitive to both details of binary interactions and stellar properties.

The mass range of CC SN progenitors can be observationally constrained by comparing the SFR (ψ) and the CC SN rate in the same galaxy sample assuming a IMF (ϕ). The simplest Poisson model formulation is to compare the total observed number of CC SNe ($N_{\rm CC}$) to the expected number ($\langle N_{\rm CC}\rangle$). The posteriori density function (PDF) can then be expressed as the Poisson probability with a prior accounting for the total observed SFR in the galaxy sample:

$$\mathcal{L} \propto \langle N_{\rm CC}\rangle^{N_{\rm CC}} \exp\left[-\langle N_{\rm CC}\rangle\right] \times \exp\left[-\frac{(\psi-\psi_{\rm obs})^2}{2\delta\psi^2}\right] \quad (6)$$

We used as estimators for the central value and scale the mean and the standard deviation of PDF and considered a flat not informative priors for the initial mass, i.e. $4 \leq m_{\rm l}^{\rm CC}/{\rm M}_\odot \leq 20$ and $20 \leq m_{\rm u}^{\rm CC}/{\rm M}_\odot \leq 100$. A different approach would have been to consider each galaxy as the source of a random process and to obtain the joint probability function as a combination of Poisson distributions. We found no statistical improvement using this variant, so we prefer to illustrate the simpler approach.

It is possible to merge the sample of SNe discovered from 1960 to 1997 by the old local SN surveys (Cappellaro et al. 1999) with that of SNe discovered in the last 13 years by properly combining the CTs of these SN surveys and the assumed CT in the last 13 years. We cross matched our galaxy samples with that from Cappellaro et al. (1999) and found 201 common galaxies with 8 CC SNe, 167 common galaxies with 8 CC SNe and 112 galaxies in common with 7 CC SNe for the sample A, B and C, respectively [7]. In our analysis we considered for each galaxy sample two

[7] The unclassified SNe have been redistributed among the three SN types according to the observed distribution: 100% type Ia in E–S0, 35% type Ia, 15% type Ib and 50% type II in spirals.

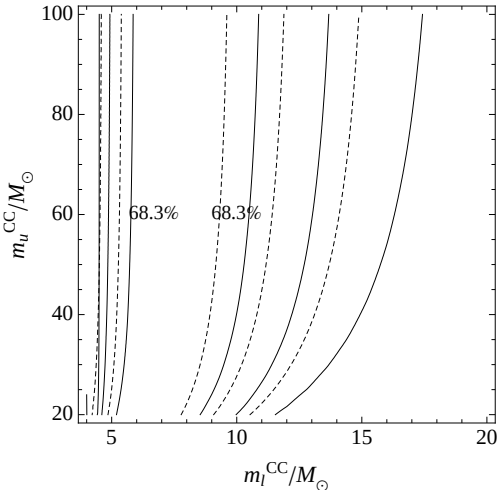

Fig. 2. Probability density function of m_l^{CC} and m_u^{CC}, after marginalization over the star formation rate, for the B sample. The contours show the 68.3%, 95.4% and 99.7% confidence limits obtained as $\mathcal{L}/\mathcal{L}_{max} = \exp -2.30/2$, $\exp -6.17/2$ and $\exp -11.8/2$, respectively. Thin and dashed lines are for $N_{CC} = 14$ and 16, respectively.

SN samples: the SNe discovered from 1998 to 2010 and the SNe discovered from 1960 to 2010. Additionally, an independent measurement of the CC SN rate in a larger galaxy sample, i.e. the estimate by Cappellaro et al. (1999) at z< 0.01, has been used as a statistical prior only for the SN sample discovered from 1998 to 2010 to further constrain the lower mass of CC SN progenitors. Results for the different galaxy and SN samples are reported in Table 3. Independent estimates obtained using different SN samples are statistically consistent and also the results in the three galaxy samples are in agreement within the uncertainties. However, the mean value obtained in the sample B is higher than those in the other two samples. In fact in the sample B we have a total SFR higher of a factor of 1.4 with respect to that in the sample A and a very similar number of SNe. The likelihood in the $m_l^{CC} - m_u^{CC}$ plane after marginalization over ψ is plotted in Fig. 2 for the sample B. As expected contours are very elongated and no significant constraint can be put on the upper limit mass of CC SN progenitors.

Table 3. Estimated minimum mass in different galaxy samples and for different SN samples. $m_{l,13}^{CC}$ has been derived considering a CT of 13 years, $m_{l,13+old}^{CC}$ has been obtained by summing 13 years and the CTs of the old SN surveys. $m_{l,13+prior}^{CC}$ has been obtained by using the estimate of the local rates as a statistical prior and a CT of 13 years.

Sample	SFR ($M_\odot yr^{-1}$)	$m_{l,13}^{CC}$ ($M_\odot$)	$m_{l,13+old}^{CC}$ ($M_\odot$)	$m_{l,13+prior}^{CC}$ ($M_\odot$)
A	$SFR_{H\alpha}$	6 ±1	6 ± 0.9	5.7±0.8
B	SFR_{UV}	8 ± 2	8.5 ± 1	8 ± 0.9
C	$SFR_{H\alpha}$	5 ±1	5 ± 0.8	5±0.7
	$SFR_{H\alpha+TIR}$	5 ±1	5 ± 0.8	6 ±0.8
	SFR_{UV}	7 ± 2	7 ± 1.5	7.5 ± 1

6. Conclusions

The massive star birth and death rates are tightly correlated due to their short lifetime and allow us to exploit the CC SN rate as a diagnostic of the current SFR by assuming the IMF and the mass range of CC SN progenitors or, conversely, to obtain a significant constrain on CC SN progenitor mass range by assuming a SFR inferred through the galaxy luminosity. Complete and volume-limited SN and galaxy samples are crucial to perform a statistically meaningful analysis and the advent of large sets of multi-wavelength observations of nearby galaxies from 11HUGS programme provide us for the first time the opportunity to compare SFRs based on CC SN rate and more established tracers in the same galaxy sample taking into account the different uncertainties and biases that affect these SFR diagnostics. We found that SFR based on $L_{H\alpha}$ can not reproduce the observed CC SN rate while there is a good agreement with the SFR based on L_{FUV} in our galaxy sample assuming a mass cutoff of 8 $M_\odot$ for CC SN progenitors and a Salpeter IMF. Thanks to multi-wavelength data set we can also compare CC SN rate and SFRs based on $L_{H\alpha}$ adopting different dust extinction corrections, from Balmer decrement or by combining TIR and Hα luminosity. Conversely, we assumed that the SFRs based on Hα and FUV luminosity are reliable and obtained an

observational constraint on the mass range of CC SN progenitors by comparing the expected number of CC SNe from SFR measurements with the observed number in our sample. Our analysis suggests that the minimum mass for CC SN progenitors is $8 \pm 1\,M_{\odot}$ and $6 \pm 1\,M_{\odot}$ if we consider FUV and Hα based SFR, respectively. The first result is in perfect agreement with that obtained by analysing a sample of nearby SNe with detected progenitor stars (Smartt et al. 2009).

Acknowledgements. It is a pleasure to acknowledge the many helpful discussions with L. Greggio and A. Pastorello.

References

Botticella, M. T., Pastorello, A., Smartt, S. J., et al. 2009, MNRAS, 398, 1041
Botticella, M. T., Riello, M., Cappellaro, E., et al. 2008, A&A, 479, 49
Brunthaler, A., Marti-Vidal, I., Menten, K. M., et al. 2010, ArXiv e-prints
Buat, V., Iglesias-Páramo, J., Seibert, M., et al. 2005, ApJ, 619, L51
Calzetti, D. 2001, PASP, 113, 1449
Cappellaro, E., Evans, R., & Turatto, M. 1999, A&A, 351, 459
Cardelli, J. A., Clayton, G. C., & Mathis, J. S. 1989, ApJ, 345, 245
Dale, D. A., Cohen, S. A., Johnson, L. C., et al. 2009, ApJ, 703, 517
Foley, R. J., Papenkova, M. S., Swift, B. J., et al. 2003, PASP, 115, 1220
Heger, A., Fryer, C. L., Woosley, S. E., Langer, N., & Hartmann, D. H. 2003, ApJ, 591, 288
Hendry, M. A., Smartt, S. J., Maund, J. R., et al. 2005, MNRAS, 359, 906
Hunter, D. J., Valenti, S., Kotak, R., et al. 2009, A&A, 508, 371
Immler, S., Brown, P., & Russell, B. R. 2010, The Astronomer's Telegram, 2639, 1
Jacques, C. & Pimentel, E. 2005, IAU Circ., 8482, 1
Karachentsev, I. D. & Makarov, D. A. 1996, AJ, 111, 794
Kennicutt, R. C., Hao, C., Calzetti, D., et al. 2009, ApJ, 703, 1672
Kennicutt, R. C. 1998, ARA&A, 36, 189
Kennicutt, Jr., R. C., Lee, J. C., Funes, José G., S. J., Sakai, S., & Akiyama, S. 2008, ApJS, 178, 247
Leaman, J., Li, W., Chornock, R., & Filippenko, A. V. 2010, ArXiv e-prints
Lee, J. C., Gil de Paz, A., Kennicutt, R. C., et al. 2010, ArXiv e-prints
Lee, J. C., Kennicutt, R. C., José G. Funes, S. J., Sakai, S., & Akiyama, S. 2009, ApJ, 692, 1305
Maguire, K., di Carlo, E., Smartt, S. J., et al. 2010, MNRAS, 404, 981
Martin, R., Yamaoka, H., Monard, L. A. G., & Africa, S. 2005, Central Bureau Electronic Telegrams, 119, 1
Monard, L. A. G. 2008a, IAU Circ., 8946, 1
Monard, L. A. G. 2008b, CBET, 1315, 1
Monard, L. A. G. 2009, CBET, 1867, 1
Nakano, S., et al. 2002, IAU Circ., 7810, 1
Pastorello, A., Kasliwal, M. M., Crockett, R. M., et al. 2008, MNRAS, 389, 955
Pastorello, A., Sauer, D., Taubenberger, S., et al. 2006, MNRAS, 370, 1752
Pozzo, M., Meikle, W. P. S., Rayner, J. T., et al. 2006, MNRAS, 368, 1169
Prieto, J. L., Bond, H. E., Kochanek, C. S., et al. 2010, The Astronomer's Telegram, 2660, 1
Pumo, M. L., Turatto, M., Botticella, M. T., et al. 2009, ApJ, 705, L138
Rich, D., et al. 2005, IAU Circ., 8497, 3
Singer, D., Pugh, H., & Li, W. 2004, IAU Circ., 8297, 2
Schlegel, D. J., Finkbeiner, D. P., & Davis, M. 1998, ApJ, 500, 525
Smartt, S. J. 2009, ARA&A, 47, 63
Smartt, S. J., Eldridge, J. J., Crockett, R. M., & Maund, J. R. 2009, MNRAS, 395, 1409
Vinkó, J., et al. 2006, MNRAS, 369, 1780
Williams, K. A., et al. 2009, ApJ, 693, 355